Published in final edited form as:
Anal Chem. 2008 March 1; 80(5): 1702–1708. doi:10.1021/ac702030f.

Quantitative Profiling of Endogenous Retinoic Acid in Vivo and in Vitro by Tandem Mass Spectrometry

Maureen A. Kane, **Alexandra E. Folias**, **Chao Wang**, and **Joseph L. Napoli***
Department of Nutritional Science and Toxicology, 119 Morgan Hall, MC#3104, University of California, Berkeley, Berkeley, California 94720-3104

Abstract

We report an improved tandem mass spectrometric assay for retinoic acid (RA) applicable to in vitro and in vivo biological samples. This liquid chromatography tandem mass spectrometric (LC/MS/MS) assay for direct RA quantification is the most sensitive to date, with a 62.5 attomol lower limit of detection and a linear range spanning greater than 4 orders of magnitude (from 250 attomol to 10 pmol). This assay resolves all-*trans*-RA (atRA) from its endogenous geometric isomers, is applicable to samples of limited size (10–20 mg of tissue), and functions with complex biological matrixes. Coefficients of variation are as follows: instrumental, ≤2.6%; intraday, 5.2% ± 0.7%; interday, 6.7% ± 0.9%. In vitro capabilities are demonstrated by quantification of endogenous RA and RA production (from retinol) in primary cultured astrocytes. Quantification of endogenous atRA and its geometric isomers in 129SV mouse serum and tissues (liver, kidney, adipose, muscle, spleen, testis, and brain) reveals in vivo utility of the assay. The ability to discriminate spatial concentrations of RA in vivo is illustrated with C57BL/6 mouse brain loci (hippocampus, cortex, olfactory bulb, thalamus, cerebellum, and striatum), as well as with Lewis rat proximal/distal mammary gland regions during various morphological stages: virgin, early pregnancy (e7), late pregnancy (e20), lactating (day 4), involuting day 1, and involuting day 11. This assay provides the sensitivity necessary for direct, endogenous RA quantification necessary to elucidate RA function, e.g., in neurogenesis, morphogenesis, and the contribution of altered RA homeostasis to diseases, such as Alzheimer's disease, type 2 diabetes, obesity, and cancer.

Metabolism activates vitamin A (retinol) into retinoic acid (RA), which controls physiological processes including development, nervous system function, immune response, cell proliferation and differentiation, and reproduction.[1–3] Expression loci of retinoid-specific binding proteins, enzymes, and receptors that contribute to RA generation, signaling, and catabolism indicate that RA concentrations in vivo are temporally/spatially controlled to produce the individual actions of vitamin A.[4–8] Recent investigations have linked alterations in retinoid metabolism to aberrant neurogenesis, aberrant mammary gland morphogenesis, and to diseases, including Alzheimer's disease, type 2 diabetes, obesity, and cancer.[9–14] These studies and others postulate alterations in RA as mechanistically important but have not quantified RA directly. Therefore, analytically rigorous measurements capable of sensitively discriminating changes in endogenous RA levels either

*To whom correspondence should be addressed. jna@berkeley.edu Phone: 510-642-5202. Fax: 510-642-0535.

spatially, and/or in response to modulation of retinoid metabolism, remain important for understanding retinoid function and its relationship to disease risk.

Resolution of isomers is important in RA analyses, as isomers of RA have different affinities for nuclear receptors and therefore may afford different biological actions. All-*trans*-RA (atRA) activates retinoic acid receptors (RAR)[15–17] and peroxisome proliferator-activated receptor, type β/δ,[18,19] whereas 9-*cis*-RA (9cRA) activates both RAR and retinoid X receptors (RXR).[20] Retinoids may exert additional biological effects through dimerization of RXR with an array of type II nuclear receptors, such as thyroid hormone, peroxisome proliferator-activated, vitamin D, liver X, farnesoid X, pregnane, constitutively activated, and the small nerve growth factor-induced clone B subfamily of nuclear receptors.[20] 13–*cis*-RA (13cRA) does not activate RAR or RXR directly but induces dyslipidemia and insulin resistance, possibly through conversion into atRA.[21–25] Tissues and serum contain 9,13-di-*cis*-RA (9,-13dcRA), which may reflect conversion from 13cRA and/or 9cRA and does not activate RAR or RXR.[26–28]

Here we report an improved and versatile method for direct quantification of atRA and its isomers in cultured cells, serum, and tissues with increased sensitivity and greater facility to monitor retinoid metabolism in vitro and in vivo. This assay provides the best sensitivity to date for quantifying RA and could be adapted to monitor RA metabolites.

EXPERIMENTAL SECTION

Materials

LC/MS grade acetonitrile and LC/MS grade water, atRA, 9cRA, and 13cRA were purchased from Sigma-Aldrich. 4,4-Dimethyl-RA was a gift from Marcia Dawson (Burnham Institute, La Jolla, CA) and Peter Hobbs (SRI International, Menlo Park, CA). 9,13dcRA was prepared as described.[26] Retinoid standards were prepared the day of use. Concentrations were verified spectrophotometrically using published ε values.[29]

Cell Culture

Hippocampus astrocytes were dissected from 2 day old Sprague–Dawley rat pups. Pups were sacrificed in a CO_2 chamber. Hippocampi were dissected from the brains, and the meninges were removed. Hippocampi were resuspended in 2 mL of Hanks' balanced salt solution (GIBCO) with 10 mM HEPES buffer, pH 8.0 and 1000 units/mL penicillin–streptomycin (GIB-CO). Individual astrocytes were mechanically dissociated by trituation though a series of Pasteur pipettes with gradually reduced diameters. Cells were plated in DMEM supplemented with 10% fetal bovine serum in 175 cm^2 tissue culture flasks and incubated in a 37 °C incubator with 5% CO_2. The medium was changed after 48 h. Cells were allowed to grow another 7–9 days until confluent. Confluent flasks were sealed and shaken at 300 rpmfor 6 h to separate oligodendrocytes and microglia cells from astrocytes. Astrocytes were recultured in 6-well plates and were incubated 5 h in the dark with all-*trans*-retinol (Sigma). The medium was aspirated, and cells were lysed on the plate with reporter lysis buffer (Promega).

Animals and Tissues

Male SV129 mice (Charles River) were fed an AIN93G diet with 4 IU/g vitamin A (vitamin A palmitate) from weaning and were bred from dams fed the same diet. Male C57BL/6 mice (Charles River) were bred from dams fed a stock diet and were fed the 4 IU of vitamin A/g from weaning. Lewis rats (Charles River) were fed a stock diet. The stock diet (Harlan Teklad Global, 18% protein rodent diet) contains 30.9 IU/g vitamin A (15.4 IU/g vitamin A acetate and 15.5 IU/g retinol). Tissues were dissected under yellow light. Brain dissections were done with a Nikon SMZ-10A dissection microscope equipped with a Volpi (Auburn, NY) NCL 150 light source with a yellow filter. Tissues were frozen in liquid nitrogen immediately after harvest and kept frozen at −80 °C until assay, within 3 days of harvest. Tissues were homogenized on ice using ground glass homogenizers (Kontes, Duall size 21) either manually or with a Heidolph motorized homogenizer (280 rpm) in cold 0.9% saline to produce a 10–25% homogenate. Serum was recovered by centrifuging clotted blood at 10 000*g* for 10 min at 4 °C. Rat mammary gland tissue was harvested from gland 4 in ~0.5 g pieces with the proximal region being closest to the nipple and the distal region including the proliferation/differentiation-rich area containing the terminal end buds. The morphological stages assayed were virgin, early pregnancy (e7), late pregnancy (e20), lactating (day 4), involuting day 1, and involuting day 11.

Extraction

Most samples were extracted with a two-step acid–base extraction that recovers multiple retinoids. Here we describe only RA quantification, but the protocol extracts retinol, retinyl ester(s), and other RA metabolites. Ten microliters of internal standard (50 nM 4,4-dimethyl-RA in acetonitrile) was added to each sample. From 1 to 3 mL of 0.025 M KOH in ethanol was added to tissue homogenates (up to 500 μL) and serum (100–200 μL). The aqueous phase was extracted with 10 mL of hexane. The organic phase containing nonpolar retinoids (retinol and retinyl ester(s)) was removed. Four molar HCl (60–180 μL) was added to the aqueous phase, and polar retinoids (RA) were removed by extraction with 10 mL hexane. Organic phases were removed under nitrogen with gentle heating at ~25–30 °C in a water bath (Organomation Associates Inc. model N-EVAP 112, Berlin, MA). RA extracts were resuspended in 60 μL of acetonitrile. Only glass containers, pipettes, and calibrated syringes were used to handle retinoids. Acetonitrile can be added during the KOH step to assist in precipitating protein that can interfere in the selected reaction monitoring (SRM) chromatograms. If only RA is quantified, a one-step acetonitrile extraction is possible. For serum (up to 200 μL), 1 mL of acetonitrile and 60 μL of 4 M HCl were added, followed by extraction with 10 mL of hexane. Measurements from 10 to 20 mg of tissue produce rigorous data from limited samples (e.g., embryo), whereas routine tissue assay amounts from adult mice range from 40 to 115 mg.

Chromatography

Two protocols were developed to resolve RA and its isomers: one predominantly for cultured cells or subcellular fractions (gradient 1) and one predominantly for tissue samples (gradient 2), which have higher background interference. Both gradients were generated with an Agilent 1100 series high-performance liquid chromatograph (HPLC) consisting of a

vacuum degasser, binary pump, temperature-controlled column compartment, and a temperature-controlled autosampler. The column compartment was maintained at 25 °C, the autosampler was maintained at 10 °C, and the injection volume was 20 μL. For both methods, a Supelcosil ABZ+PLUS Supelguard cartridge column (Supelco, 2.1 mm × 20 mm, 5 μm) preceded the analytical column: A, H_2O with 0.1% formic acid; B, acetonitrile with 0.1% formic acid. Gradient 1 (cultured cell/subcellular fraction protocol) separation was effected with a Supelcosil ABZ+PLUS column (Supelco, 2.1 mm × 100 mm, 3 μm) at 400 μL/min with the following linear gradient: 0–5 min, 60% B to 95% B; 5–8 min, hold at 95% B; 8–9 min, 5% B to 60% B; 9–12 min, re-equilibrate with 60% B. Gradient 2 (tissue protocol) separation was effected with an Ascentis RP-Amide column (Supelco, 2.1 × 150 mm, 3 μm) at 400 μL/min with the following linear gradient: 0–3 min, hold at 70% B; 3–15 min, 70% B to 95% B; 15–20 min, hold at 95% B; 20–21 min, 5% B to 70%B; 21–25 min, re-equilibrate at 70% B.

Tandem Mass Spectrometry (MS/MS)

Data were acquired with an Applied Biosystems API-4000 triple-quadrupole mass spectrometer equipped with APCI (atmospheric pressure chemical ionization) operated in positive ion mode. The instrument was controlled by Analyst v1.4 software and was operated in multiple reaction monitoring mode. RA was monitored using an *m*/*z* 301.1 $[M + H]^+$ to *m*/*z* 205.0 transition, whereas 4,4-dimethyl-RA was monitored using an *m*/*z* 329.4 $[M + H]^+$ to *m*/*z* 151.3 transition. The dwell time for both RA and 4,4-dimethyl-RA was 150 ms. Optimum positive APCI conditions included the following: collision gas, 7; curtain gas, 10; gas1, 70; nebulizer current, 3; source temperature, 350; declustering potential, 55; entrance potential, 10; collision energy, 17; collision exit potential, 5. Data from previous work was acquired with an Applied Biosystems API-3000 triple-quadrupole mass spectrometer equipped with APCI using the conditions described.[30]

RESULTS AND DISCUSSION

MS/MS

In APCI, analyte ionization occurs through gas-phase ion–molecule reactions at atmospheric pressure using the evaporated mobile phase as the ionizing gas to yield $[M + H]^+$. Several reports have shown that positive APCI has numerous advantages for RA analysis, including favorable ionization efficiency based on the conjugated structure and carboxylic acid group (Figure 1), greater sensitivity and lower background than negative APCI, and greater signal intensity and linear dynamic range than electrospray ionization.[30–32] Selected reaction monitoring of transitions characteristic of analyte decomposition reactions were used to provide specificity and sensitivity. Product ions, produced by collisionally activated precursor ion fragmentations with N_2, were examined for intensity and background levels. The most intense transition with the lowest accompanying background was *m*/*z* 301.1 → 205.0 for RA and *m*/*z* 329.4 → 151.3 for 4,4-dimethyl-RA. The reduction in background provided by monitoring a specific precursor-to-product ion transition, in which the analyte must meet two distinct *m*/*z* requirements, is illustrated for atRA (Figure 2). A scan of Q1 shows significant background, whereas a Q3 scan of product ions obtained from the collisionally activated decomposition of the precursor RA ion exhibits a >1000-fold

decrease in background. This reduction in background contributes to the sensitivity of this method, especially with complex matrixes.

Endogenous RA concentrations in the samples illustrated in the current work were orders of magnitude below the limit of detection (LOD) and/or limit of quantification (LOQ) for both diode array (DAD) and single-wavelength UV detection. Therefore, the suggestion that DAD can be used as a routine codetector with MS/MS to confirm peak identity overlooks the very large sensitivity differences between the two techniques and, thus, eliminates the rationale for progressing from optical to MS detection.[33] If DAD or single-wavelength UV had the sensitivity to quantify endogenous RA in readily accessible sample sizes, there would be limited need for the more expensive and complex MS/MS.

Chromatography

We verify peak identity/instrument performance daily by injecting a mixture of authentic RA standards. Within the course of a given analysis, retention times remain stable within ±0.1 min. Shifts in chromatographic retention times in this work and our previous work result only from routine reconfiguration, such as using different lengths of connective tubing, presence or absence of a guard column, and/or presence or absence of protective frits before the analytical column.

Mobile phase composition was designed to optimize resolution of RA isomers and signal intensity. Acetonitrile/water/0.1% formic acid produced optimum sensitivity and resolution for the instrument used in this work (API-4000). Formic acid in the mobile phase prevents peak distortion from partially dissociated carboxylic acid groups and facilitates protonation in positive APCI. Note that mass spectrometric sensitivity is both mobile phase and instrument/design dependent and should be verified empirically. For example, our previous work, done with a different instrument (API-3000), produced optimum sensitivity with methanol/water/0.1% formic acid.[30] This mobile phase, however, did not provide optimum resolution. Therefore, we used an acetonitrile/methanol/water/0.1% formic acid mixture as a compromise between resolution and sensitivity. In the current protocol(s), the acetonitrile/water/0.1% formic acid mobile phase composition optimizes both resolution and signal intensity.

We developed two different gradients that resolve RA isomers: atRA, 9RA, 9,13dcRA, 13cRA (Figure 3). It is important to resolve these RA isomers from atRA and each other, because all four occur either endogenously and/or in metabolically altered/challenged states in humans and/or animals.[26–28,30,34] Recent reports of LC/MS methods limited to serum/plasma that separate only 13cRA from atRA would produce inflated values for one or both, because 9,13dcRA (and if present, 9cRA) comigrate with 13cRA and/or atRA.[33,35] Gradient 1 (12 min run time) provides slightly better sensitivity in half the analysis time, relative to gradient 2. Gradient 1 works well with cultured cell extracts, subcellular fractions, or samples with a less complex matrix, such as serum (Figure 3A). Rigorous analyses of tissue extracts require gradient 2 (25 min run time), which also can be used for “gradient 1” type samples (Figure 3B). Interfering substances present in complex matrixes shifted in gradient 2 to chromatographic regions that did not overlap with retinoids of interest.

Sample Preparation

Samples should be harvested and extracted under yellow light. A yellow or red filter prevents RA isomerization and degradation in samples prepared with a dissecting microscope. Tissues not extracted immediately should be frozen immediately after harvest in liquid N_2 and stored whole at −80 °C until assay. Tissues and/or serum can be stored up to 1 week at −80 °C without significant retinoid degradation. Tissues should be thawed on ice immediately before homogenization and should be homogenized on ice and extracted immediately. Homogenized samples will undergo significant degradation after 2 h at 4 °C from matrix effects.[30,34] Samples should not be frozen, thawed, and then refrozen. Contamination of the hexane layer with the acid-containing aqueous layer should be avoided to prevent acid-catalyzed isomerization and degradation of retinoids. Resuspended samples remain stable in a cooled autosampler (in amber vials, under yellow lights) for several days. Resuspended samples can be stored at −20 °C for 1 week without significant retinoid degradation. The internal standard, 4,4-dimethyl-RA, serves to assess handling losses, extraction efficiency, and handling-induced isomerization. Typical average recoveries (± SEM) ranged from 80% ± 11% (tissues, $n = 40$) to 95% ± 4% (serum, $n = 20$). Rigorous data can be generated on ~10–20 mg of tissue (wet weight).

Performance

Assay performance was assessed for sensitivity, linearity, and reproducibility. Lower LOD and LOQ provide sensitivity measures. The LOD, defined here as a signal-to-noise ratio of 3, and the LOQ, defined here as a signal-to-noise ratio of 10, determined for both gradient 1 and gradient 2 are shown (Figure 4). Gradient 1 has an LOD of 62.5 attomol (0.0625 fmol) and an LOQ of 250 attomol (0.25 fmol) for atRA. LOD/LOQ for 9cRA and 13cRA were 125 attomol (0.125 fmol)/1 fmol and 1 fmol/4 fmol, respectively, for gradient 1. Gradient 2 has an LOD of 125 attomol (0.125 fmol) and an LOQ of 750 attomol (0.750 fmol) for atRA. LOD/LOQ for 9cRA and 13cRA were 125 attomol (0.125 fmol)/1 fmol and 2 fmol/6 fmol, respectively, for gradient 2. This method provides the best sensitivity to date for detection and quantification of RA, with a 20-fold lower LOD than our previous work[30] and a 13–300-fold lower LOD than other published methods.[32–38]

A representative calibration curve for atRA using gradient 1 shows the extensive linear dynamic range (Figure 5). Note the agreement to the best fit line below 50 fmol. Similar curves were generated for gradient 2 and for the other geometric isomers with both gradients. Linear working ranges extend from 0.25 to 6 fmol (depending on analyte lower LOQ) to 1–10 pmol (upper LOQ). Correlation coefficients, r^2, exceeded 0.999.

Repeat measurements of standards on the same day assess assay precision (instrumental coefficient of variation, ≤2.6%) and accuracy (agreement between applied and measured amounts, >95%). Intra-assay (5.2% ± 0.7%, $n = 6$) and interassay coefficients of variation (6.7% ± 0.9%, $n = 6$) were determined with multiple aliquots (solid pieces) from the same liver analyzed on the same day and consecutive days.

The sample preparation described here, although not extensive, purifies the matrix sufficiently to enhance accuracy and the lives of guard and analytical columns. Attention to

sample preparation also provides dividends in sensitivity and accuracy, especially in the low-femtomole range. The simpler sample preparations available are adequate only for samples with less complicated matrixes, such as serum from normal subjects, or certain cell culture extracts.[33,35,38,39] Most tissues (e.g., liver, kidney, testis, etc.) and/or serum from metabolically altered subjects present a more complex matrix, which requires sufficient matrix cleanup to prevent deterioration of assay performance. The sample preparation protocol reported here was designed to quantify atRA and its isomers in the low-femtomole range, regardless of the type of sample assayed, and allows analysis of greater than 5–10 000 samples (~6–12 months) before requiring column replacement. Methods that shorten sample preparation modestly require changing guard columns daily and replacing analytical columns frequently, even with the relatively simple matrix of normal serum.[35]

Application

We show the versatility of this assay by successful application to both in vitro (cultured cell) and in vivo (mouse/rat) models used to study retinoid metabolism. Data from primary rat astrocytes illustrates the in vitro utility of the assay with small numbers of cultured cells. Individual measurements of endogenous atRA in cells (typically $4–5 \times 10^5$ astrocytes per well in a 6-well plate) and their medium (~1 mL aliquot) were achieved readily (Figure 6). Representative SRM chromatograms of RA produced from treatment of astrocytes with 0.1 μM retinol are shown. In the assay described previously,[30] endogenous RA and RA produced and retained within astrocytes incubated with 0.1 μM retinol were not detectable. Additionally, previous data of RA secreted into the medium upon incubation with 0.1 μM retinol was detectable but below the LOQ. Here, endogenous RA was quantifiable. RA produced and retained within the astrocytes or secreted into the medium was readily measured for all retinol concentrations (Figure 6). This method provides a powerful in vitro assay tool with sensitivity that allows for treatment of cell systems with low levels of retinoids and has been/will be applied to a number of primary culture and transfected cell lines to study retinoid metabolism and enzyme action.

Quantification of endogenous RA in vivo is essential for elucidating normal retinoid function as well as assessing the contribution of altered retinoid homeostasis to various disease/metabolically challenged states. Representative SRM chromatograms of endogenous RA in mouse liver (~40 mg tissue) and serum (~150 μL) show the in vivo utility of the assay with small biological samples (Figure 7). The assay was applied to quantify RA reference values from tissues of SV129 mice fed an AIN93G purified diet with 4 IU of vitamin A/g, bred from dams maintained on the same diet (Table 1), or from brain and brain regions of C57BL/6 mice fed an AIN93G purified diet with 4 IU of vitamin A/g from weaning, but bred from dams fed standard lab chow (≥30 IU of vitamin A/g) (Table 2). The 2-fold difference in total brain atRA between the offspring of dams fed either a 4 IU of vitamin A/g or stock diet (>30 IU of vitamin A/g) indicates that copious dietary vitamin A in the dam continues to affect retinoid homeostasis even in offspring fed a recommended amount of vitamin A. The RA data in Table 1, except testis, are higher than reported previously for mice fed a stock diet.[30] Excessive vitamin A induces RA-metabolizing CYP enzymes, resulting in increased formation of polar metabolites of RA and depressed endogenous levels of RA in tissues. The sensitivity of tissues to altered dietary vitamin A was variable,

with RA differences ranging from none (testis) to increases of 50% (serum), 2-fold (kidney), and 4-fold (liver and brain). The unaltered testis RA values are likely due to isolated retinoid production/metabolism, as well as to relatively high steady-state levels of CYP26A1. These data illustrate the impact of dietary vitamin A levels, not only on retinyl esters, but also on RA. Copious dietary vitamin A likely confounds the retinoid “metabolome”, which evolved to concentrate and conserve scarce vitamin A.

Retinoids function with temporal–spatial selectivity, which requires the ability to quantify spatial RA concentrations within a given tissue.[3–11] In addition to the brain loci data (Table 2), we quantified atRA from sections of mammary gland to illustrate the assay’s utility in distinguishing spatial and temporal concentrations of RA (Figure 8). Mammary gland was chosen because it undergoes extensive morphological changes during development, consistent with those mediated by retinoids, such as epithelial differentiation, proliferation, and apoptosis.[11] For example, impairing RAR function causes aberrant proliferation and differentiation in the mammary gland, which responds to treatment with exogenous RA.[11] We measured the proximal and distal regions of rat mammary gland at various stages of gland development. Here, we identified differences in RA among morphological stages, as well as spatial differences between regions at specific morphological stages. RA increased 20–35% in both proximal and distal regions during early pregnancy (e7) relative to virgin glands. During late stages of pregnancy (e20), the distal region had RA levels significantly below virgin (−20%) and early pregnancy (−35%). RA in the proximal region remained elevated. During lactation and on involution day 1, RA returned to levels comparable to that of virgin. On involution day 11, however, the distal region had 25% less RA than the proximal region and 17% less than the virgin gland. Serum RA in rats did not change, except for involution day 1, which was ~42% greater than during lactation. Such direct measurements of spatially controlled RA concentrations will greatly assist in assessing the role of RA in morphological changes and represent a significant improvement in quantitative analytical methodology over previous indirect and/or nonspecific RA detection techniques.

SUMMARY

This specific LC/MS/MS assay for direct quantification of RA demonstrates improved sensitivity and applicability to in vitro and in vivo systems. The benefits of LC/MS/MS relative to other detection methods have been reviewed.[30] LC coupled with tandem MS does not require retinoid derivatization and offers increased sensitivity and specificity relative to LC/UV, LC/electrochemical detection, GC/MS, LC/fluorescence, and LC/MS. This report offers rigorous quantification of atRA and biologically occurring isomers. Other methods claim simultaneous measurement of retinoids in addition to RA but were applied only to simple matrixes, such as plasma, serum, or cultured cells.[33,35] Currently, no assays have been reported that simultaneously quantify the wide range of endogenous retinoids, including retinyl esters, retinol, retinal, RA, numerous polar metabolites (4-oxo, 4-OH, 18-oxo, etc.), di(dehydro)retinoids (e.g., 3,4-didehydro-RA and –retinol and others), and glucuronidation products. Multiple issues contribute to the lack of a universal assay, including vast differences in analytes’ chromatography, sensitivities to pH, and concentrations in vivo.

Methods of quantifying RA in normal human serum were developed 20 years ago,[36,39,40–42] and reliable methods for quantifying endogenous RA in tissues were developed recently.[30,34,40] LC/MS/MS methods with the increased sensitivity shown in this work are needed to elucidate retinoid function, e.g., in neurogenesis, morphogenesis, and to study RA homeostasis during diseases, such as Alzheimer's disease, type 2 diabetes, obesity, and cancer. The LC/MS/MS assay reported here for direct RA quantification is the most sensitive to date, has improved applicability for in vitro and in vivo samples, functions well with complex matrixes, and has been demonstrated to be useful with the small samples used to distinguish spatial distributions of RA in vivo.

Acknowledgments

This work was supported by NIH Grants DK36870, AG13566, DK46839 and an NIH Kirschstein Individual Fellowship F32 DK066924 (M.A.K.).

References

1. Wolf G. Physiol. Rev. 1984; 64:873–937. [PubMed: 6377341]
2. Mark M, Ghyselinck ND, Chambon P. Annu. Rev. Pharmacol. Toxicol. 2006; 46:451–480. [PubMed: 16402912]
3. Maden M. Proc. Nutr. Soc. 2001; 59:65–73. [PubMed: 10828175]
4. Ruberte E, Friederich V, Chambon P, Moriss-Kay G. Development. 1991; 111:45–60. [PubMed: 1849812]
5. Ong DE. Nutr. Rev. 1994; 52:S24–S31. [PubMed: 8202279]
6. Yamagata T, Momoi MY, Yanagisawa M, Kumagai H, Yamakado M, Momoi T. Brain Res. Dev. Brain Res. 1994; 77:163–176.
7. Krezel W, Kastner P, Chambon P. Neuroscience. 1999; 89:1291–1300. [PubMed: 10362315]
8. Harrison EH. Annu. Rev. Nutr. 2005; 25:87–103. [PubMed: 16011460]
9. McCaffery PJ, Adams J, Maden M, Rosa-Molinar E. Eur. J. Neurosci. 2003; 18:457–472. [PubMed: 12911743]
10. Jacobs S, Lie DC, DeCicco KL, Shi Y, DeLuca LM, Gage FH, Evans RM. Proc. Natl. Acad. Sci. U.S.A. 2006; 103:3902–3907. [PubMed: 16505366]
11. Wang YA, Shen K, Wang Y, Brooks SC. Dev. Dyn. 2005; 234:892–899. [PubMed: 16217742]
12. Goodman AB, Pardee AB. Proc. Natl. Acad. Sci. U.S.A. 2003; 100:2901–2905. [PubMed: 12604774]
13. Goodman AB. J. Cell. Physiol. 2006; 209:598–603. [PubMed: 17001693]
14. Graham TE, Modey N, Preitner F, Peroni OD, Zabolotny JM, Kotani K, Quadro L, Kahn BB. Nature. 2005; 436:356–362. [PubMed: 16034410]
15. Sucov HM, Evans RM. Mol. Neurobiol. 1995; 10:169–184. [PubMed: 7576306]
16. Szeto W, Jiang W, Tice DA, Rubinfeld B, Hollingshead PG, Fong SE, Dugger DL, Pham T, Yansura DG, Wong TA, Grimaldi JC, Corpuz RT, Singh JS, Frantz GD, Devaux B, Crowley CW, Schwall RH, Eberhard DA, Rastelli L, Polakis P, Pennica D. Cancer Res. 2001; 61:4197–4205. [PubMed: 11358845]
17. Chambon P. FASEB J. 1996; 10:940–954. [PubMed: 8801176]
18. Shaw N, Elholm M, Noy N. J. Biol. Chem. 2003; 278:41589–41592. [PubMed: 12963727]
19. Schug TT, Berry DC, Shaw NS, Travis SN, Noy N. Cell. 2007; 129:723–733. [PubMed: 17512406]
20. Germain P, Chambon P, Eichele G, Evans RM, Lazar MA, Leid M, De Lera AR, Lotan R, Mangelsdorf DJ, Gronemeyer H. Pharmacol. Rev. 2006; 58:760–772. [PubMed: 17132853]
21. Bershad S, Rubinstein A, Paterniti JR, Le NA, Poliak SC, Heller B, Ginsberg HN, Fleischmajer R, Brown WV. N. Engl. J. Med. 1985; 313:981–985. [PubMed: 2931603]

22. Rodondi N, Darioli R, Ramelet A-A, Hohl D, Lenain V, Perdrix J, Wietlisbach V, Riesen WF, Walther T, Medinger L, Nicod P, Desvergne B, Mooser V. Ann. Intern. Med. 2002; 136:582–589. [PubMed: 11955026]
23. Heliovaara MK, Remitz A, Reitamo S, Teppo A-M, Karonen S-L, Ebeling P. Metab. Clin. Exp. 2007; 56:786–791. [PubMed: 17512311]
24. Staels B. J. Am. Acad. Dermatol. 2001; 45:S158–S167. [PubMed: 11606948]
25. McCormick AM, Kroll KD, Napoli JL. Biochemistry. 1983; 22:3933–3940. [PubMed: 6577913]
26. Arnhold T, Tzimas G, Wittfoht W, Plonait S, Nau H. Pharmacol. Lett. 1996; 59:169–177.
27. Horst RL, Reinhardt TA, Goff JP, Nonnecke BJ, Gambhir VK, Fiorella PD, Napoli JL. Biochemistry. 1995; 34:1203–1209. [PubMed: 7827070]
28. Horst RL, Reinhardt TA, Goff JP, Koszewski NJ, Napoli JL. Arch. Biochem. Biophys. 1995; 322:235–239. [PubMed: 7574681]
29. Barua AB, Furr HC. Mol. Biotechnol. 1998; 10:167–182. [PubMed: 9819815]
30. Kane MA, Chen N, Sparks S, Napoli JL. Biochem. J. 2005; 388:363–369. [PubMed: 15628969]
31. McCaffery P, Evans J, Koul O, Volpert A, Reid K, Ullman MD. J. Lipid Res. 2002; 43:1143–1149. [PubMed: 12091499]
32. Wang Y, Chang WY, Prins GS, van Breeman RB. J. Mass Spectrom. 2001; 36:882–888. [PubMed: 11523087]
33. Ruhl R. Rapid Commun. Mass Spectrom. 2006; 20:2497–2504. [PubMed: 16862622]
34. Schmidt CK, Brouwer A, Nau H. Anal. Biochem. 2003; 315:36–48. [PubMed: 12672410]
35. Gundersen TE, Bastani NE, Blomhoff R. Rapid Commun. Mass Spectrom. 2007; 21:1176–1186. [PubMed: 17330217]
36. Napoli JL. Methods Enzymol. 1986; 123:112–124. [PubMed: 3702709]
37. Meyer E, Lambert WE, De Leenheer AP, Bersaques JP, Kint AH. J. Chromatogr. 1991; 570:149–156. [PubMed: 1839158]
38. Sakhi AK, Gundersen TE, Ulven SM, Blomhoff R, Lundanes E. J. Chromatogr., A. 1998; 828:451–460. [PubMed: 9916324]
39. De Leenheer AP, Lambert WE, Claeys I. J. Lipid Res. 1982; 23:1362–1367. [PubMed: 7161564]
40. Lampen A, Meyer S, Arnhold T, Nau H. J. Pharmacol. Exp. Ther. 2000; 295:979–985. [PubMed: 11082432]
41. Napoli JL, Pramanik BC, Williams JB, Dawson MI, Hobbs PD. J. Lipid Res. 1985; 26:387–392. [PubMed: 3989394]
42. Arafa HM, Hamada FM, Elmazar MM, Nau H. J. Chromatogr., A. 1996; 729:125–136. [PubMed: 9004933]

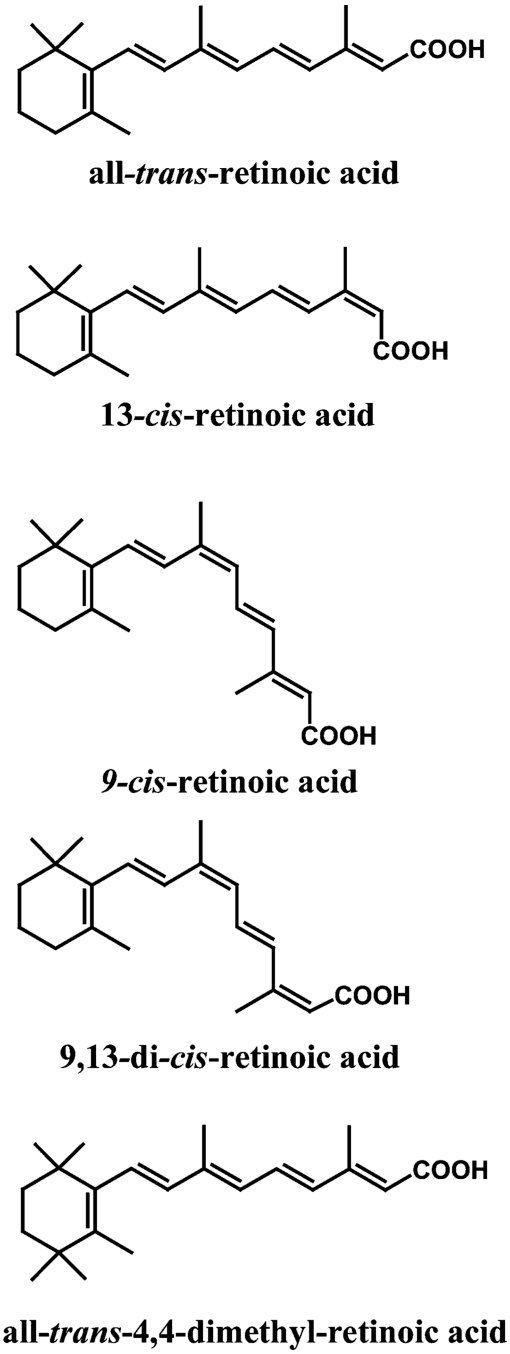

Figure 1.
Structures of atRA, its isomers, and the internal standard 4,4-dimethyl-RA.

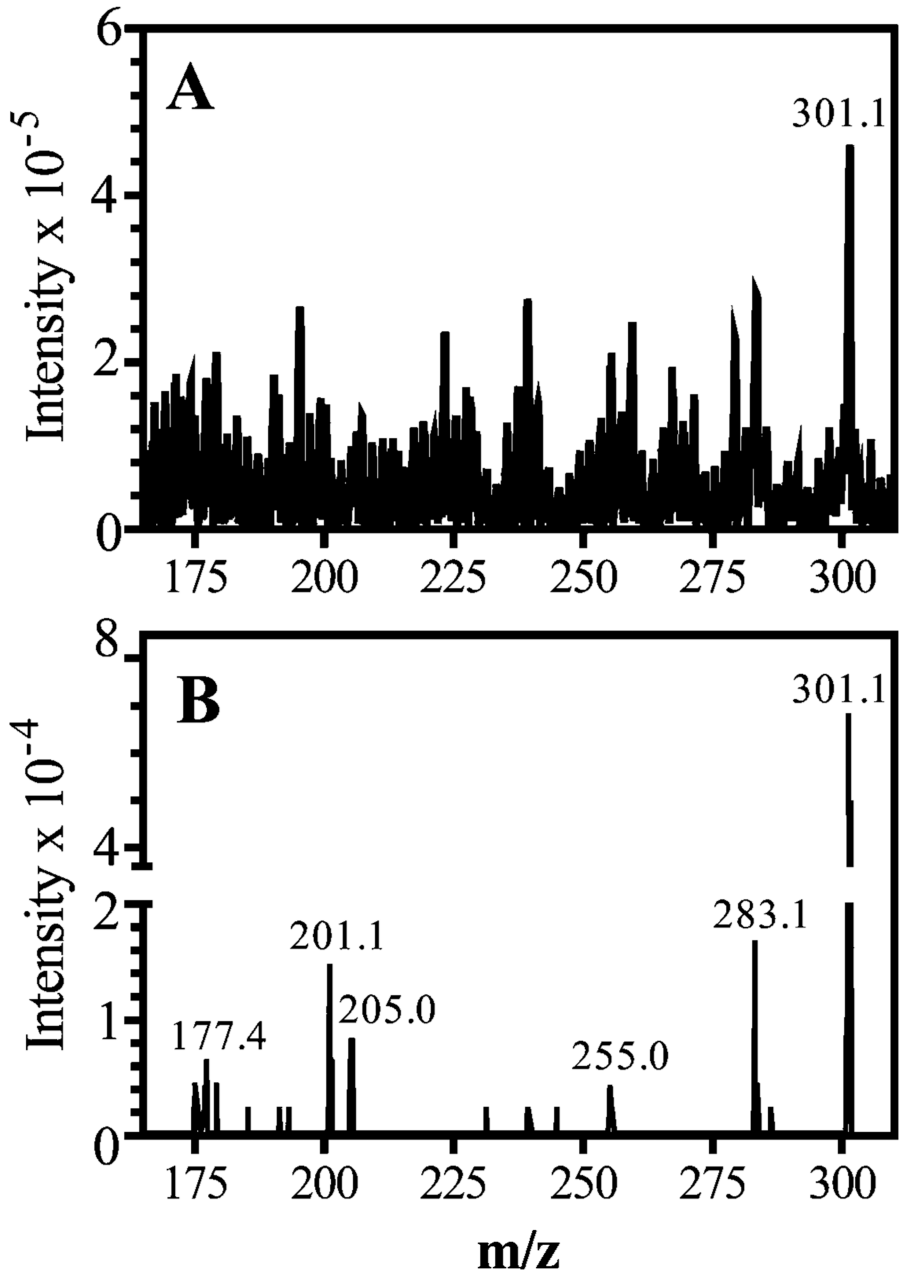

Figure 2.

RA mass spectra. (A) Q1 scan showing $[M + H]^+$ (*m*/*z*: 301.1). (B) Q3 scan showing $[M + H]^+$ and product ions obtained after fragmentation. Both scans were obtained by infusing 200 nM RA at 10 μL/min. Note the reduction in background in (B).

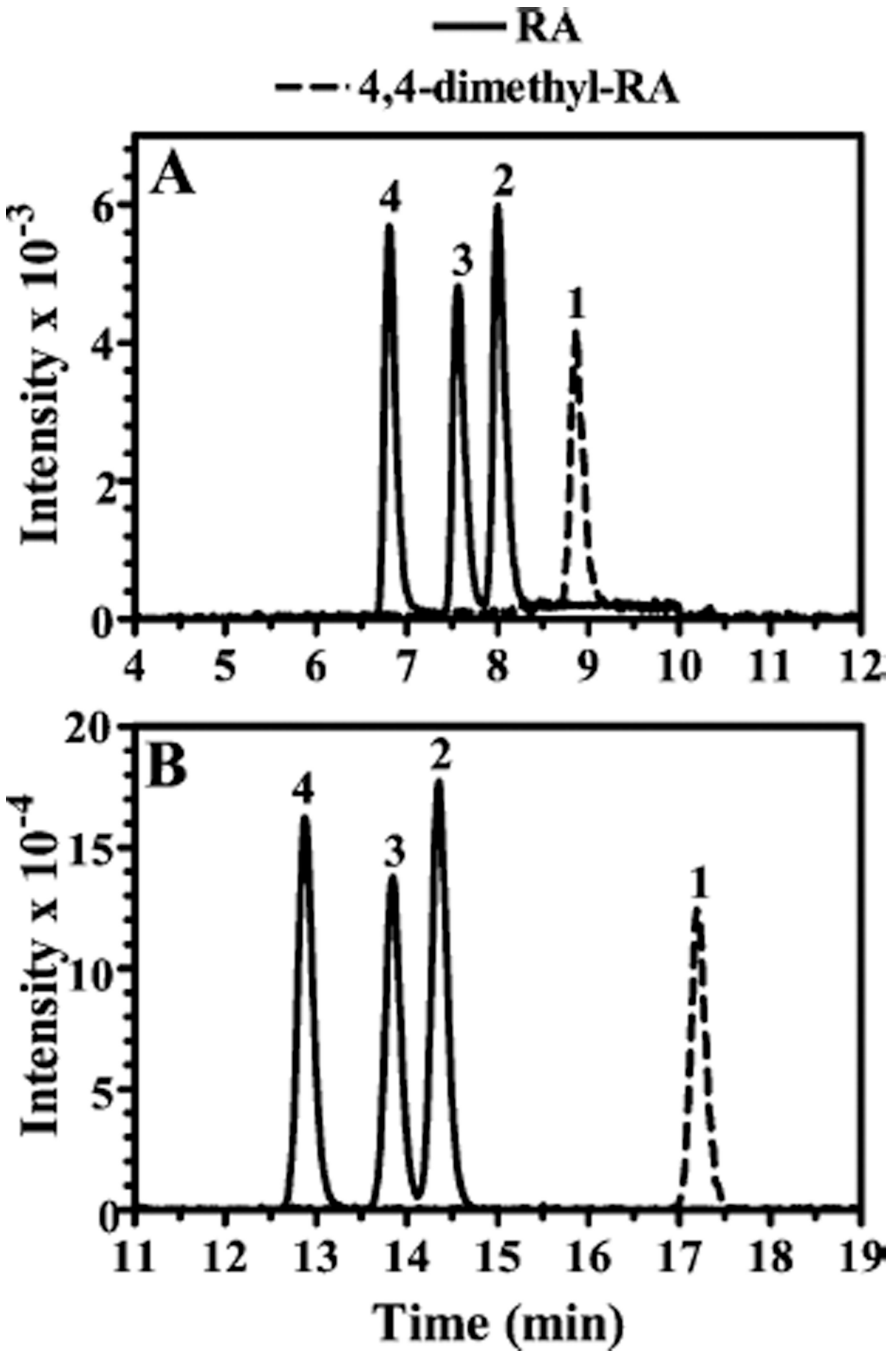

Figure 3.

SRM chromatograms of standard solutions: (A) gradient 1, cultured cell/subcellular fraction protocol; (B) gradient 2, tissue protocol. The solid line corresponds to *m*/*z* Q1:301/Q3:205, and the broken line corresponds to *m*/*z* Q1:329/Q3:151: 1, 4,4-dimethyl-RA; 2, atRA; 3, 9cRA; 4, 13cRA. 9,13-dcRA elutes between 3 and 4 (data not shown).

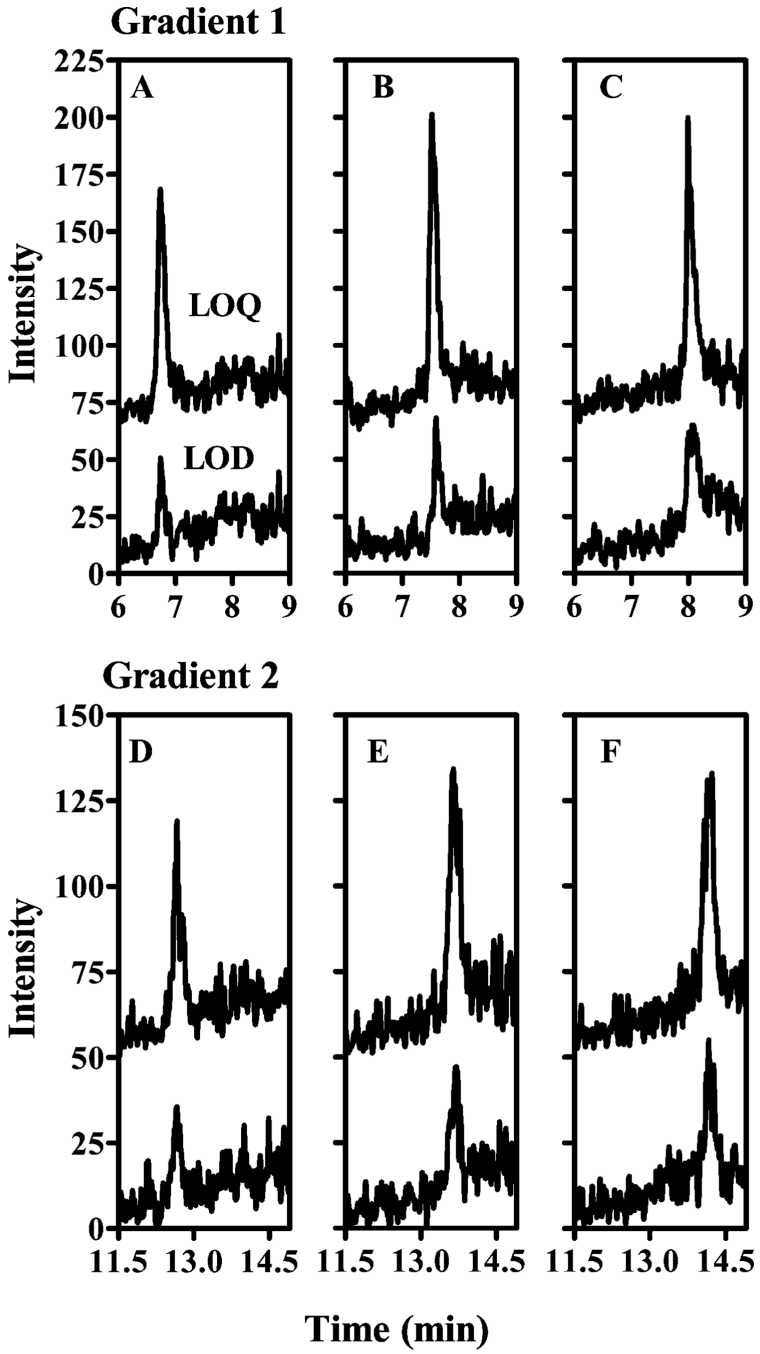

Figure 4.

LOD and LOQ for (A–C) gradient 1, cultured cell/subcellular fraction protocol, and (D and F) gradient 2, tissue protocol. (A and D) 13cRA. (B and E) 9cRA. (C and F) atRA.

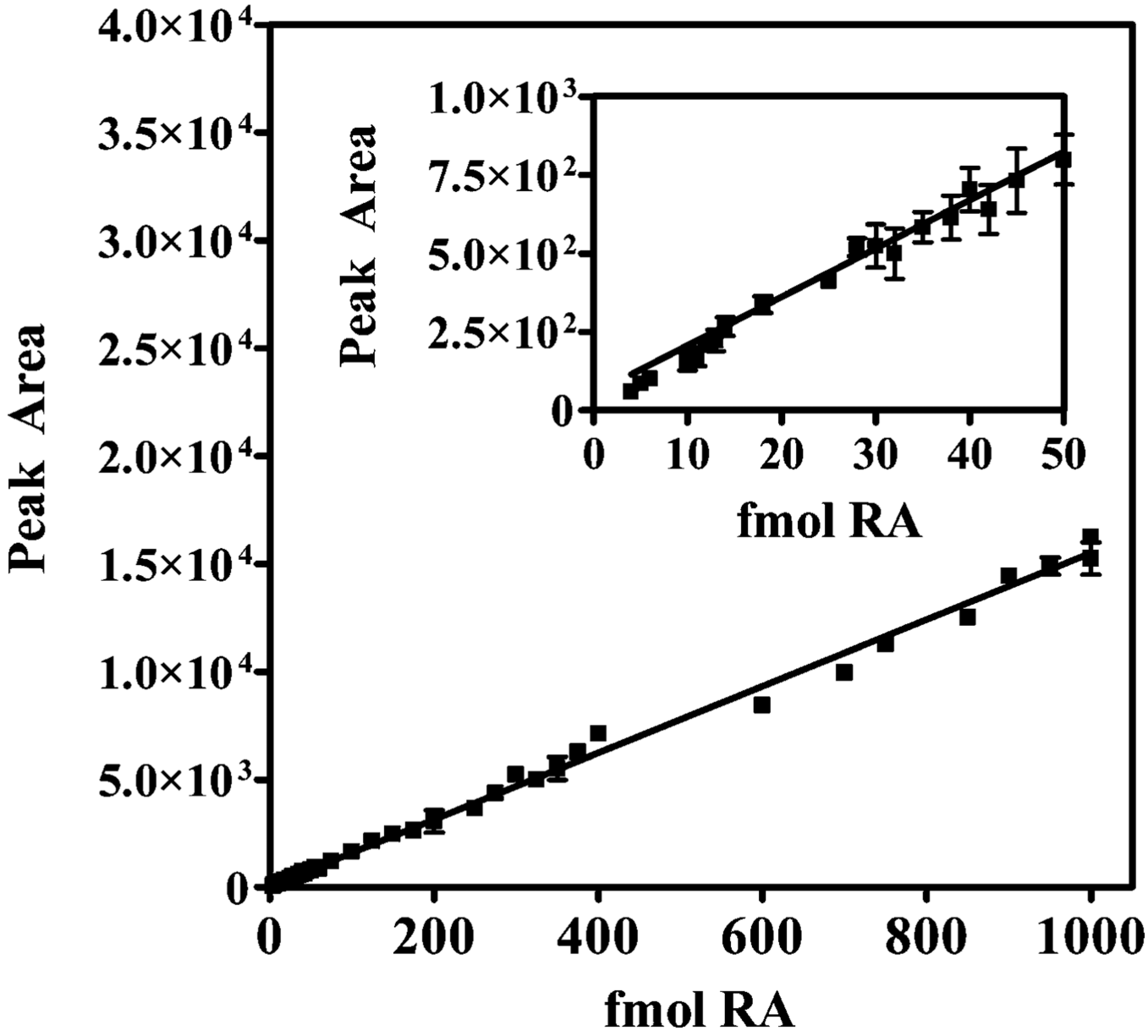

Figure 5.

Representative calibration curve for atRA. Data were obtained using the cultured cell protocol (r^2, 0.999). Similar curves were generated for the tissue protocol and for the other geometric isomers with both protocols. Note the functionality of the assay with values of <50 fmol (inset).

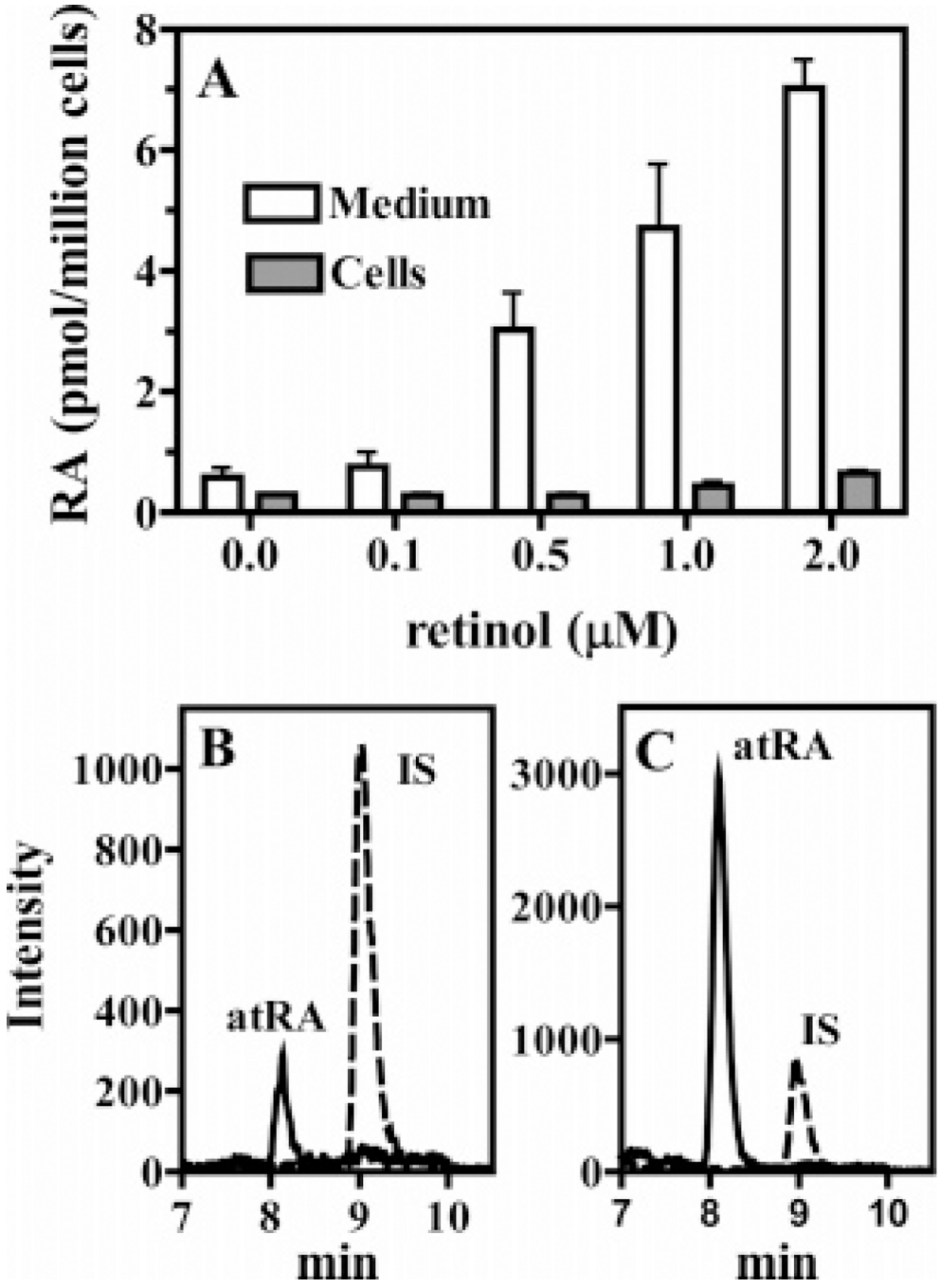

Figure 6.

Quantification of endogenous atRA and atRA biosynthesis in primary cultures of hippocampus astrocytes. (A) Data were generated using gradient 1 after 5 h of incubation with retinol. Data are averages of triplicates. (B and C) Representative SRM chromatograms of RA in cells and medium, respectively, after incubation with 0.5 μM retinol: IS, internal standard.

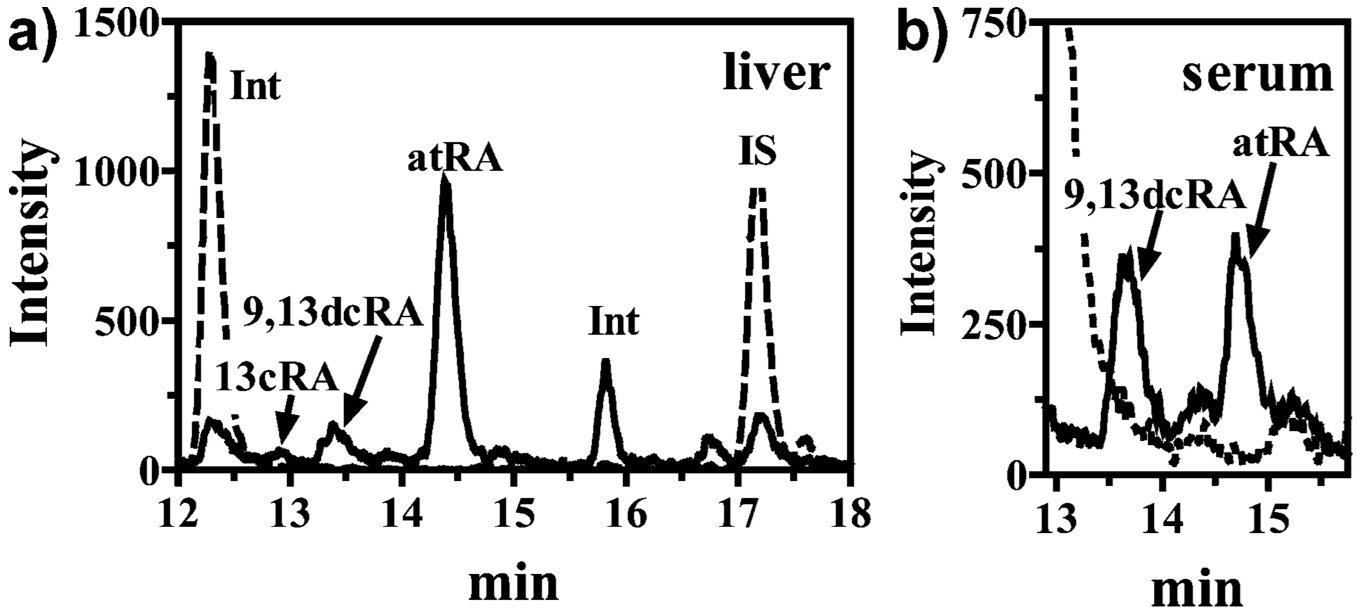

Figure 7.

Representative SRM chromatograms of endogenous RA. Data were generated with gradient 2. (A) Analysis of liver extract (~40 mg of tissue) from 2–4 month old, male 129SV mice fed 4 IU/g vitamin A. (B) Serum (~150 μL) from the same mice. The solid line represents RA (*m*/*z* Q1:301/Q3:205); the dashed line represents the IS 4,4-dimethyl-RA (*m*/*z* Q1:329/Q3:151). INT, nonspecific signal.

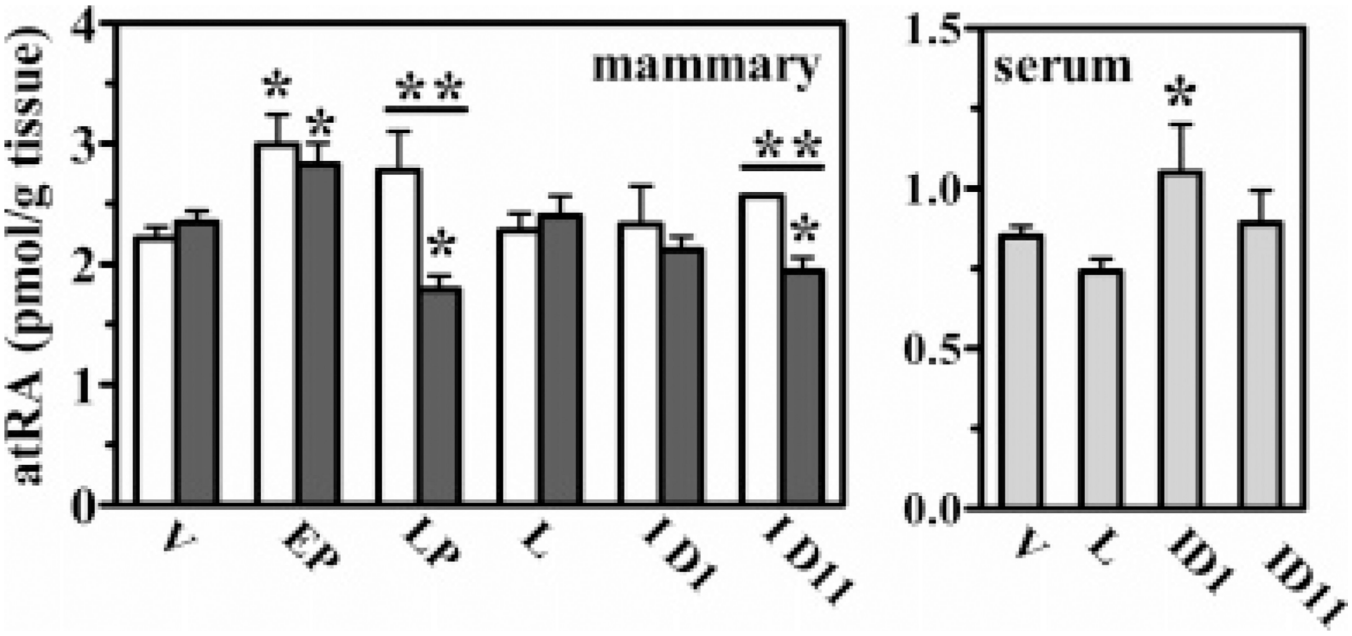

Figure 8.

Quantification of atRA in rat mammary gland. Open bars show atRA in the proximal region; filled bars show atRA in the distal region. Also shown are serum measurements. Samples were collected from female Lewis rats fed a stock diet: V, virgin; EP, early pregnancy (e7); LP, late pregnancy (e20); L, lactation (day 4); ID1, involution day 1; ID11, involution day 11. *$P < 0.05$, compared to virgin (mammary) or compared to L (serum); **$P < 0.05$ between proximal and distal. Data are means ± SD, $n = 3–13$ samples.

Table 1

Endogenous RA in Mouse Tissues[a]

serum/tissue	atRA	9-*cis*-RA	9,13-di-*cis*-RA	13-*cis*-RA
serum	2.7 ± 0.3 (21)	n.d.	1.6 ± 0.3 (15)	1.1 ± 0.1 (19)
liver	38.1 ± 3.4 (18)	n.d.	23.0 ± 1.3 (5)	6.2 ± 1.0 (7)
kidney	15.2 ± 2.2 (30)	n.d.	12.1 ± 1.6 (20)	5.7 ± 2.2 (9)
adipose (epididymal)	14.2 ± 2.4 (18)	n.d.	4.5 ± 0.6 (29)	1.1 ± 0.2 (7)
muscle	1.5 ± 0.2 (15)	n.d.	n.d.	1.0 ± 0.1 (7)
spleen	7.3 ± 0.6 (14)	n.d.	3.3 ± 0.4 (9)	4.7 ± 0.2 (8)
testis	8.9 ± 1.0 (14)	n.d.	4.3 ± 0.4 (5)	2.6 ± 0.6 (6)
brain	17.1 ± 3.7 (19)	n.d.	18.2 ± 3.0 (21)	3.0 ± 0.6 (10)

[a]Data were generated from 2–4 month old male SV129 mice fed, and bred from dams fed, an AIN93G diet with 4 IU of vitamin A/g. Values are means ± SEM (*n*) expressed as pmol/g tissue.

Table 2

Endogenous RA in Mouse Brain and Brain Regions[a]

region	atRA	9-*cis*-RA	9,13-di-*cis*-RA	13-*cis*-RA
whole brain	33.9 ± 3.9 (8)	n.d.	20.6 ± 2.6 (8)	22.2 ± 1.1 (4)
hippocampus	45.3 ± 5.2 (8)	n.d.	21.1 ± 1.3 (8)	23.8 ± 3.1 (8)
cortex	16.0 ± 1.3 (7)	n.d.	17.2 ± 1.9 (7)	30.3 ± 2.5 (7)
olfactory bulb	76.5 ± 21.3 (4)	n.d.	19.8 ± 2.4 (4)	38.1 ± 5.6 (4)
thalamus	80.9 ± 6.0 (4)	n.d.	22.4 ± 2.0 (4)	46.3 ± 1.9 (4)
cerebellum	54.8 ± 3.6 (8)	n.d.	17.6 ± 1.1 (8)	42.3 ± 4.8 (4)
striatum	78.0 ± 33.2 (3)	n.d.	25.2 ± 11.1 (3)	33.4 ± 11.2 (3)

[a]Data were generated from 4 month old male C57BL/6 mice fed an AIN93M diet with 4 IU of vitamin A/g from weaning and bred from dams fed a stock diet (>30 IU of vitamin A/g). Values are means ± SEM (*n*), expressed as pmol/g tissue.